Antiviral Research 83 (2009) 228–237

Contents lists available at ScienceDirect

Antiviral Research

journal homepage: www.elsevier.com/locate/antiviral

Translational insensitivity to potent activation of PKR by HCV IRES RNA

Takashi Shimoike[a], Sean A. McKenna[b], Darrin A. Lindhout[c], Joseph D. Puglisi[c,*]

[a] Department of Virology II, National Institute of Infectious Diseases, Musashi-murayama, Tokyo 208-0011, Japan
[b] Department of Chemistry, University of Manitoba, Winnipeg, MB R3T 2N2, Canada
[c] Department of Structural Biology, Stanford University School of Medicine, Stanford, CA 94305-5126, USA

ARTICLE INFO

Article history:
Received 9 December 2008
Received in revised form 25 March 2009
Accepted 7 May 2009

Keywords:
PKR
Translation
HCV
IRES
eIF2

ABSTRACT

Translation of hepatitis C virus (HCV) is initiated at an internal ribosome entry site (IRES) located at the 5′end of its RNA genome. The HCV IRES is highly structured and greater than 50% of its nucleotides form based-paired helices. We report here that the HCV IRES is an activator of PKR, an interferon-induced enzyme that participates in host cell defense against viral infection. Binding of HCV IRES RNA to PKR leads to a greatly increased (20-fold) rate and level (4.5-fold) of PKR autophosphorylation compared to previously studied dsRNA activators. We have mapped the domains in the IRES required for PKR activation to domains III–IV and demonstrate that the N-terminal double-stranded RNA binding domains of PKR bind to the IRES in a similar manner to other RNA activators. Addition of HCV IRES RNA inhibits cap-dependent translation in lysates via phosphorylation of PKR and eIF2α. However, HCV IRES-mediated translation is not inhibited by the phosphorylation of PKR and eIF2α. The results presented here suggest that hydrolysis of GTP by eIF2 is not an essential step in IRES-mediated translation. Thus, HCV can use structured RNAs to its advantage in translation, while avoiding the deleterious effects of PKR activation.

1. Introduction

Viral RNAs control key aspects of both viral and host function. Beyond their function as genomic material, viral RNAs can act as *cis*-regulatory elements, as binding sites for proteins or other nucleic acids and their complexes. Hepatitis C virus (HCV) is a positive-sense RNA virus of the flaviviridae family and is the main causative agent of chronic hepatitis, cirrhosis, and hepatocellular carcinoma (Guidotti and Chisari, 2006). Translation of the HCV genome is initiated using an RNA element at its 5′end, known as an internal ribosome entry site (IRES) (Tsukiyama-Kohara et al., 1992; Wang et al., 1993). The host 40S ribosomal subunit binds directly to the IRES with high affinity, positioning the IRES start codon proximally to the ribosomal peptidyl-tRNA site (P-site) where the initiator tRNA codon–anticodon interaction forms (Otto and Puglisi, 2004; Pestova et al., 1998). The cap binding and scanning activities of a subset of initiation factors, including eIF4E and eIF4G, are not required for HCV IRES-mediated initiation (Otto and Puglisi, 2004; Pestova et al., 1998; Reynolds et al., 1996). IRES-40S complex formation leads to subsequent stepwise assembly of translationally competent complexes. Only a subset of host translation factors is required for HCV IRES-mediated initiation, including initiator $tRNA^{Met}$, the trimeric GTPase eIF2, as well as the IF2 orthologous eIF5B, another GTPase, and the large multiprotein assembly eIF3 (Ji et al., 2004; Otto and Puglisi, 2004; Pestova et al., 1998). Hydrolysis of GTP by eIF2 or eIF5B gates downstream events leading to assembly of the 80S initiation complex and translation of the HCV viral proteins (Locker et al., 2007; Pestova et al., 2001; Terenin et al., 2008).

The HCV IRES is highly structured and conserved among viral genotypes. The IRES contains a large fraction of based-paired secondary structure, with over 50% of the 372 nts involved in Watson–Crick or G–U pairing (Honda et al., 1999; Zhao and Wimmer, 2001). The secondary structure of the IRES consists of 4 structural domains rich in double-helical regions (domains I–IV) (Fig. 1A). Structural features of these domains have been determined using NMR spectroscopy and X-ray crystallography (Kieft et al., 2002; Kim et al., 2002; Lukavsky et al., 2000, 2003). The functional and structural roles of these domains in IRES mediated translation have been defined; domain I is thought to be dispensable for IRES function, whereas domains II–IV form the functional core. Domain III directs high-affinity contact with a protein-rich ribosomal surface near the tRNA exit site (E site) (Kieft et al., 2001; Kolupaeva et al., 2000; Lytle et al., 2001; Otto et al., 2002; Otto and Puglisi, 2004). The domain IIIabc junction, stem loop IIIe, and the RNA pseudoknot are essential for ribosomal interaction. Domain II is located near the ribosomal P-site codon, and likely modulates factor binding and function (Locker et al., 2007).

* Corresponding author. Tel.: +1 650 498 4397.
E-mail address: puglisi@stanford.edu (J.D. Puglisi).

0166-3542/$ – see front matter © 2009 Published by Elsevier B.V.
doi:10.1016/j.antiviral.2009.05.004

Host response to double-stranded RNAs is a hallmark of innate immunity. Double-stranded RNA-dependent protein kinase (PKR) is central to this response (Gale and Katze, 1998). PKR is a 551 amino acid protein, containing tandem double-stranded RNA binding domains (dsRBDs) at the N-terminus and a C-terminal serine-threonine kinase domain, connected by a flexible 80 amino acid linker (Clemens and Elia, 1997). Both dsRBDs are required for PKR binding to and activation by dsRNA (Bevilacqua and Cech, 1996; Kim et al., 2006; McKenna et al., 2007d). Upon RNA binding, self-association of PKR facilitates autophosphorylation of PKR at a key threonine in a canonical activation loop (Dey et al., 2005; McKenna et al., 2007d; Wu and Kaufman, 1997). The phosphorylated, catalytically active form of PKR regulates protein synthesis via efficient substrate phosphorylation of the α-subunit of eukaryotic initiation factor 2 (eIF2α) at Ser51, inhibiting the guanine nucleotide exchange activity of the eIF2 heterotrimeric complex and resulting in a reduction in translation efficiency (Gale and Katze, 1998).

Long stretches of double-stranded RNA are unusual in host RNAs. However, viral RNAs can be rich in secondary structure to accommodate packing into capsids. In addition, double-stranded RNAs can be formed during viral replication as intermediates. To probe how PKR responds to structured viral RNAs, we have investigated the activation of PKR by the HCV IRES. Here we show that the HCV IRES is an extremely potent activator of PKR kinase activity. We have mapped the domains in the IRES required for activation to domains III–IV, which mediate interaction of the IRES with the ribosome, and demonstrated that the dsRBDs of PKR bind to the IRES in a similar manner as to other RNA activators. We show that addition of HCV IRES RNA to translation extracts leads to potent inhibition of canonical cap-mediated translation. However, HCV IRES-initiated translation is not affected by PKR-mediated eIF2 phosphorylation. Thus, HCV is able to use structured RNAs to its advantage in translation, while avoiding the deleterious effects of PKR activation.

2. Materials and methods

2.1. Plasmid architecture

Plasmids for transcription of HCV IRES, pT7HCVIRES (J1), (JFH-1), (H77c), and (S52) carry the cDNA of nucleotides 1–374 of HCV J1 (genotype 1b), JFH-1(2a), H77c(1a), and S52(3a) under a T7 promoter, respectively. A PCR product containing, in order, a HindIII site, T7 promoter, HCV IRES sequence, BsmBI site, and EcoRI site was cloned into HindIII and EcoRI sites of pUC118. Plasmids for the transcription of HCV IRES domains, pT7II, pT7III–IV, pT7IIIb, pT7IIIacd, and pT7IIIef-IV carry cDNA of nucleotides 45–117, 119–354, 178–221, (137–178 and 221–287), and (119–139 and 285–354) of HCV J1were designed as above, with the exception that the BsmBI and EcoRI sites are replaced with a BsaI site for domain II and BbsI site for domains III–IV, IIIb, IIIacd, and IIIef–IV.

DNA fragments for luciferase reporter RNAs are under the control of a T7 promoter; pT7HCVLuc carries nucleotides 1-374 (5′UTR and 33nt of core protein-coding region of HCV J1) and nucleotides 9372-9549 (3′UTR) of HCV J1 at the 5′ and 3′end of the firefly luciferase gene, respectively. pT7EMCVLuc contains EMCV IRES (nucleotides 271–831) at the 5′end of Firefly luciferase gene (Shimoike et al., 1999). pT7HCVLuc, pT7EMCVLuc, and pRL-null that carry the Renilla luciferase gene under control of a T7 promoter (Promega) are linearized with BamHI, XhoI, and XbaI, respectively.

2.2. RNA and protein preparation

For the preparation of HCV IRES (J1, JFH-1, H77c, and S52), II, III–IV, IIIIb, IIIacd, IIIef–I, TAR (Kim et al., 2006), and VA_I RNA (McKenna et al., 2006), pT7HCV IRES, II, III–IV, IIIb, IIIacd, IIIef-IV, pTAR, and pVA_I were linearized with BsmBI (HCV IRES), BsaI (II, VA_I), BbsI (III–IV, IIIb, IIIacd, IIIef-IV), or BstZI (TAR), respectively. All viral RNAs were prepared via *in vitro* transcription as described

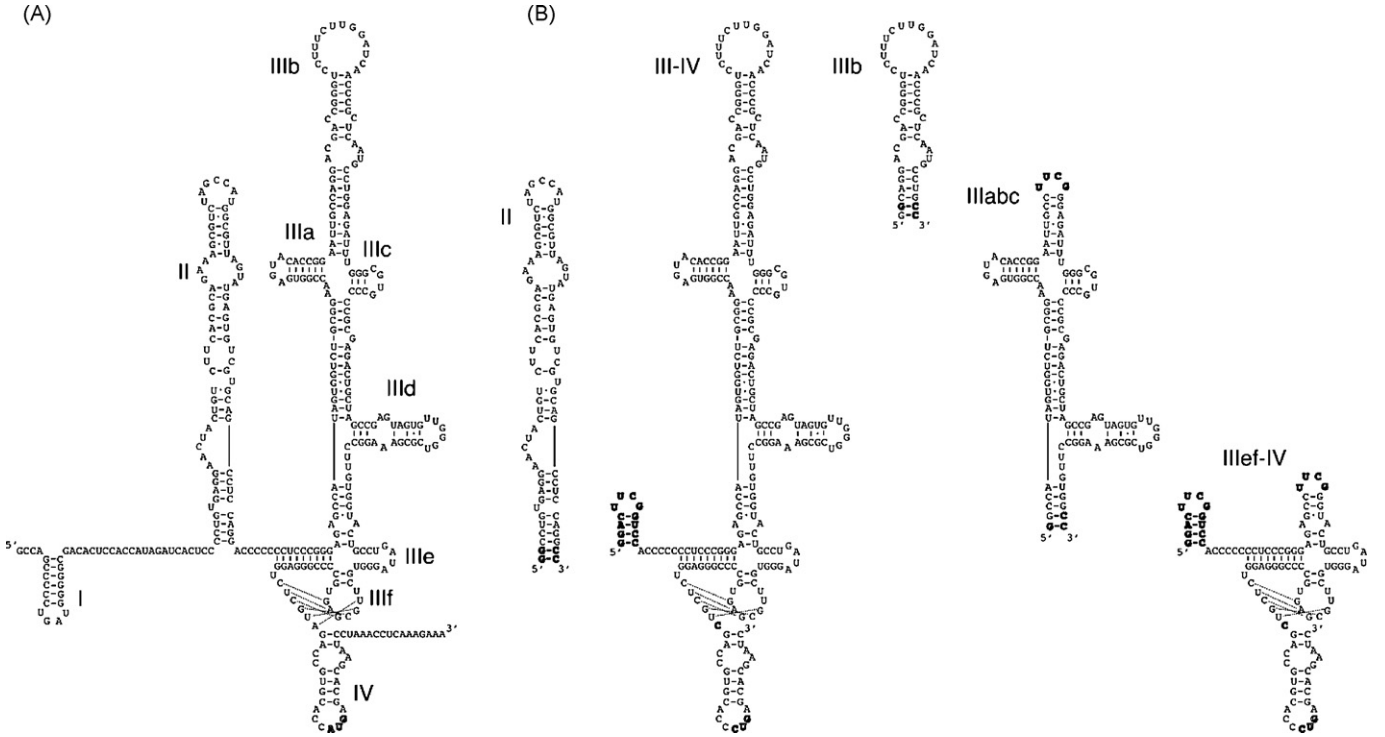

Fig. 1. Sequences and secondary structures of HCV IRES RNA. (A) Predicted secondary structure of HCV 5′UTR and immediately downstream the open reading frame (denoted as "HCV IRES", 1–374 nts) (Honda et al., 1999; Zhao and Wimmer, 2001). Individual stem-loop structures are indicated by roman numerals, and the translation initiation codon (AUG) is highlighted in bold font. (B) Truncations of HCV IRES RNA employed, including domain II (II), domains III and IV (III–IV), domain IIIb (IIIb), domains IIIa, IIIc, and IIId (IIIacd), and domains IIIe, IIIf, and IV (IIIef–IV). Nucleotide modifications to stabilize the secondary structure of each construct are indicated in bold.

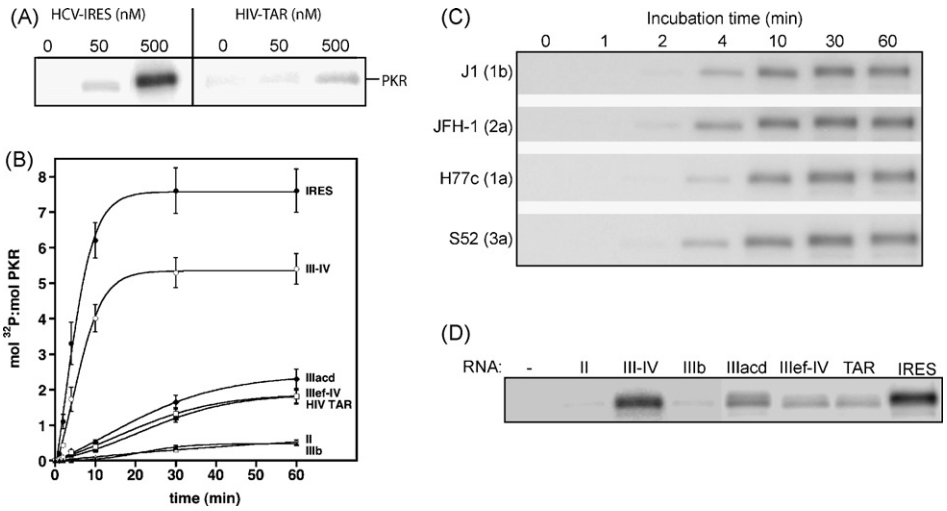

Fig. 2. HCV IRES is a potent activator of PKR autophosphorylation. In all cases, reaction components are resolved by SDS-PAGE, and the extent of PKR autophosphorylation is quantified by autoradiography. (A) Purified PKR (500 nM) incubated with HCV IRES or HIV TAR RNA activator in the presence of [γ-^{32}P]-ATP at 30 °C for 1 h. (B) Progress curves of PKR autophosphorylation where PKR (200 nM) was incubated in the presence of HCV IRES, HCV IRES domain truncations, and HIV-TAR (300 nM). Each time point was performed at least in triplicate, with error bars representing the standard deviation from the mean result. (C) Purified PKR (200 nM) incubated with IRES elements from four distinct HCV genotypes (1b, 2a, 1a, and 3a; 300 nM) in the presence of [γ-^{32}P]-ATP at 30 °C for 0, 1, 2, 4, 10, 30, and 60 min. (D) Purified PKR (200 nM) incubated in the presence of HCV IRES, HCV IRES domain truncations, and HIV-TAR (300 nM).

in detail elsewhere (McKenna et al., 2007a). It should be noted that this approach eliminates perfectly duplexed RNA that may have been generated as a result of transcription from a linearized plasmid.

Reporter RNAs, HCV FLuc, EMCV FLuc, and cap-RLuc for *in vitro* translation experiments were transcribed *in vitro* using T7 polymerase at 37 °C for 2 h, incubated with DNase (Ambion) at 37 °C for 20 min, and purified by buffer-exchange with HPLC H_2O (J.T. Baker) using a Vivaspin2 concentrator (10 kDa MWCO, Vivascience).

The purification of PKR, mutant K296R PKR and dsRBDs is described extensively elsewhere (McKenna et al., 2007c). For the *in vitro* translation, buffer in which purified PKR and mutant K296R PKR contain was exchanged with 50 mM Tris–HCl pH7.5, 100 mM KCl, 5 mM β-mercapto ethanol by Vivaspin concentrator (30 kDa MWCO, Vivascience).

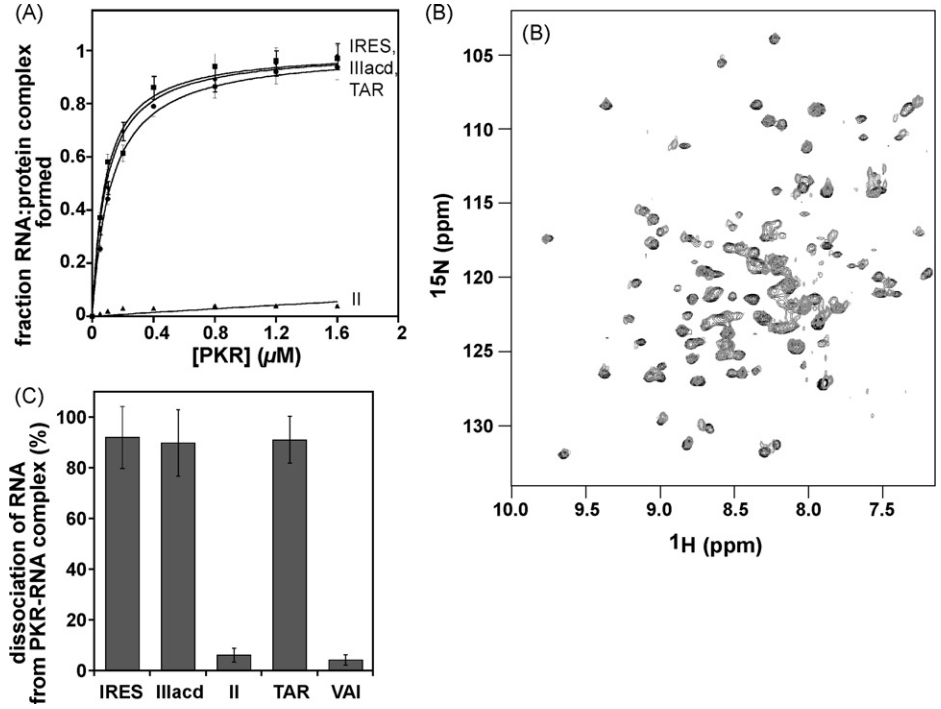

Fig. 3. Affinity of PKR for HCV IRES RNA. (A) Native gel-shift mobility assays, where HCV IRES, IIIacd, II, or HIV TAR RNA (200 nM) was incubated with an increasing amount of the dsRBDs of PKR (residues 1–169), were performed. Protein–RNA complexes were separated on non-denaturing TBE gels (5% or 10%) and stained with 1× SybrGreenII fluorescent dye for quantitation. (B) Superposition of ^{1}H-^{15}N TROSY NMR spectra of uniformly ^{15}N-labeled dsRBDs in complex with either IIIacd (grey) or HIV TAR RNA (black). (C) PKR–RNA complexes were pre-assembled (200 nM), and incubated at 30 °C for 0 or 60 min in the presence or absence of ATP and $MgCl_2$. RNA dissociation was quantified by resolving reaction components on non-denaturing TBE gels (5% or 10%) and dsRNA staining by SybrGreenII. Each data point represents at least a triplicate measurement, with the associated standard deviation shown.

2.3. Autophosphorylation assays

All autophosphorylation assays were performed as described previously (McKenna et al., 2006). Kinetics experiments were analyzed using Berkeley Madonna X (version 8.3.12) software to fit the differential equations that describe a bimolecular model of PKR activation as discussed elsewhere (McKenna et al., 2007d).

2.4. In vitro translation assay

HeLa cell S10 lysate was prepared from HeLa-S3 cells (National Cell Culture Center) with the methods described previously (Otto and Puglisi, 2004), with the following exception; 60 mM KCl was used to obtain the translations initiated by HCV IRES, or EMCV IRES and by cap.

HCV FLuc, EMCV FLuc, or capped RLuc were incubated with purified PKR in HeLa cell S10 lysate (50% volume) in 50 mM Tris–HCl pH7.5, 1 mM $MgCl_2$, 1 mM ATP, 60 mM KCl, 25 μM amino acid mixture (Promega), 0.5 U/μl SUPERase In RNase inhibitor (Ambion) at 30 °C for 1 h. The translational efficiencies were measured by using Dual-Luciferase Reporter Assay System (Promega) and Luminometer (Analytical Luminescence Laboratory).

2.5. Western blotting

Immobilon-P Transfer membrane (Millipore) was incubated with primary antibody; anti-p-PKR (446T, sc16565R, Santa Cruz Biotechnology), anti-PKR (sc6282, Santa Cruz Biotechnology), anti-p-eIF2α (Ser-51, ab4837, Abcam), or anti-eIF2α (ab5369, Abcam), and then with secondary antibody, Immun-Star GAM-HRP conjugate, or Immun-Star GAR-HRP conjugate (Bio-Rad). The membrane filters were incubated with ECL western blotting detection reagents (GE Healthcare), and exposed to X-ray Hyperfilm (GE healthcare).

2.6. NMR spectroscopy

All NMR samples were prepared to final volumes of approximately 225 μl and performed as described previously (McKenna et al., 2007d).

2.7. Native gel-shift mobility assay

All samples were prepared and run as described elsewhere (McKenna et al., 2007d).

3. Results

3.1. HCV IRES RNA is a potent activator of PKR autophosphorylation

Secondary-structure predictions and determinations demonstrated a highly structured HCV IRES element (Fig. 1A) (Honda et al., 1999; Kieft et al., 2002; Kim et al., 2002; Lukavsky et al., 2000, 2003; Zhao and Wimmer, 2001). We therefore hypothesized that the IRES should interact with and activate PKR. We first determined whether HCV IRES stimulates PKR autophosphorylation. Using well-established protocols for RNA synthesis and purification in our laboratory, we ensured that IRES RNA was chemically and conformationally homogenous (McKenna et al., 2007a). Purified full-length HCV IRES RNA was incubated with purified PKR in the buffer containing ATP, [γ^{32}-P]-ATP and Mg^{2+}. As expected, in the absence of RNA ligand no significant phosphorylation of PKR was observed (Fig. 2A). Inclusion of HCV IRES RNA in the reaction resulted in significant PKR autophosphorylation, establishing a maxima when equimolar amounts of PKR and HCV IRES were mixed. HCV IRES RNA leads to a higher plateau level of multiple phosphates per mole of PKR compared with HIV TAR activation (Fig. 2A). Similar levels of autophosphorylation were detected when comparing HCV IRES and poly I:C RNA, although a quantitative comparison was not possible due the heterogeneous composition of the poly I:C reagent (data not shown).

PKR autophosphorylation in the presence of dsRNA often proceeds via a bimolecular reaction mechanism (McKenna et al., 2007b,d). To test whether HCV IRES follows this previously observed reaction scheme, we probed the kinetics of autophosphorylation. A sigmoidal buildup of product was observed with a short lag phase prior to maximal rates of PKR autophosphorylation, and fitted well with a simple bimolecular reaction scheme (Fig. 2B, IRES). A maximal rate of autophosphorylation was observed within 5 min of HCV IRES RNA addition, and the reaction was complete in less than 30 min. When compared to HIV TAR RNA, a known viral activator of PKR (Kim et al., 2006; McKenna et al., 2007d), HCV IRES RNA leads to a faster rate of autophosphorylation and a higher plateau level of multiple phosphates per mole of PKR.

Despite the high conservation of HCV IRES sequence, various HCV genotypes may introduce nucleotide variations that affect PKR

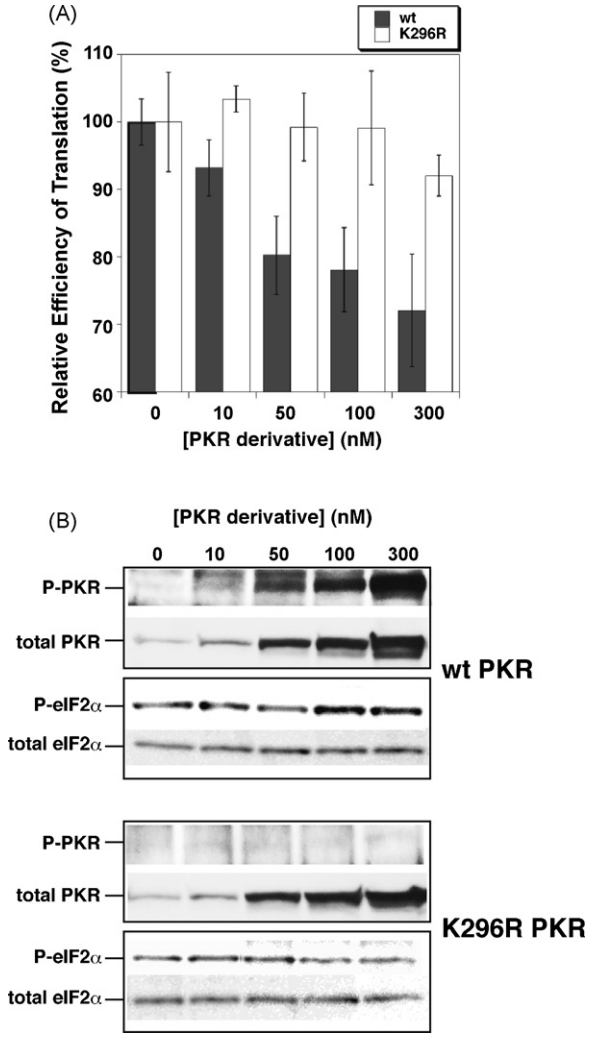

Fig. 4. Cap-dependent translation is inhibited by PKR autophosphorylation. Capped RLuc (50 nM) was incubated with HCV IRES RNA (100 nM) and increasing amounts of either wild-type PKR or catalytically inactive mutant K296R. The relative efficiency of translation was determined in HeLa cell S10 lysate with a 1 h incubation at 30 °C. After incubation portions of the same reaction mixture were used to determine (A) translational efficiency (via luciferase assay) and (B) phosphorylation state (by Western blotting). Standard deviations are shown from experiments repeated in at least triplicate. Note that the *y*-axis begins at 60% for comparison purposes.

activation. PKR autophosphorylation was monitored using IRES elements from four distinct HCV genotypes (Fig. 2C). Regardless of genotype, similar levels of PKR autophosphorylation were observed at all time points examined.

3.2. Intact domains III and IV are necessary for maximal PKR activation by HCV IRES

We then explored the structural requirements within the IRES for PKR activation. A minimum dsRNA duplex length of only 16–18 bp is required for high-affinity interaction between the dsRBDs and dsRNAs (Bevilacqua and Cech, 1996; Kim et al., 2006). As the length of the HCV IRES far exceeds this requirement, a specific domain of HCV IRES may mediate the activation of PKR. To test this hypothesis, five constructs of HCV IRES RNA were transcribed and purified (Fig. 1B); we have previously characterized the folding and function of these domains (Kim et al., 2002; Lukavsky et al., 2000, 2003; Otto et al., 2002). The stimulation of PKR autophosphorylation by each construct was monitored as above.

Truncation of the IRES by removal of domain I or domains I and II have only a minor effect on IRES-stimulated autophosphorylation. Domain II in isolation, which adopts a long helix interrupted by internal loops, multi-nucleotide bulges and non-canonical base pairs, does not significantly activate PKR (Fig. 2D). Intact domains III–IV are required for efficient stimulation of PKR autophosphorylation as deletions within this domain attenuate the plateau level of autophosphorylation. Autophosphorylation kinetics confirms the importance of domains III and IV; both the plateau level of phosphorylation of PKR and the rate of autophosphorylation are significantly attenuated for deletions within domain III–V (Fig. 2B).

A simple bimolecular reaction scheme fits the kinetic data, indicating that the HCV IRES, its domain truncations, and TAR all employ a similar reaction mechanism to activate PKR. Both HCV IRES and III–IV achieve maximal rates of autophosphorylation within 5 min of RNA addition, and achieve reaction completion in less than 30 min (Fig. 2B). Conversely, HIV TAR, IIIacd, and IIIef–IV require 15–30 min to achieve maximal rate of autophosphorylation, and do not achieve completion until well after 1 h. These results confirm the supposition that domains III and IV are crucial to the activation process, and that a fundamental structural or electrostatic feature of the full-length IRES leads to potent autophosphorylation of PKR.

3.3. Affinity of PKR for HCV IRES RNA

Domains III and IV of HCV IRES are crucial for stimulation of PKR activity, as demonstrated by the deletion mutants, above. To probe whether a change in affinity for PKR was responsible for this effect, native RNA gel-shift mobility assays were performed. Quantitative determination of complex formation was performed, and binding curves established for the interaction between HCV IRES, IIIacd, and HIV TAR with PKR (Fig. 3A). Regardless of the RNA moiety employed, roughly equivalent binding curves were obtained, with nearly equivalent dissociation constants (K_D) 93 ± 7, 125 ± 12, and 83 ± 8 nM determined for HCV IRES, HCV-IIIacd, and HIV-TAR, respectively. Therefore, a difference in an affinity of RNA for PKR does not appear to lead to different levels of PKR autophosphorylation. Domain II oligonucleotide binds with much weaker affinity to the dsRBDs of PKR ($K_D = 8.9 \pm 0.8$ μM), consistent with the lack of PKR activation by this domain.

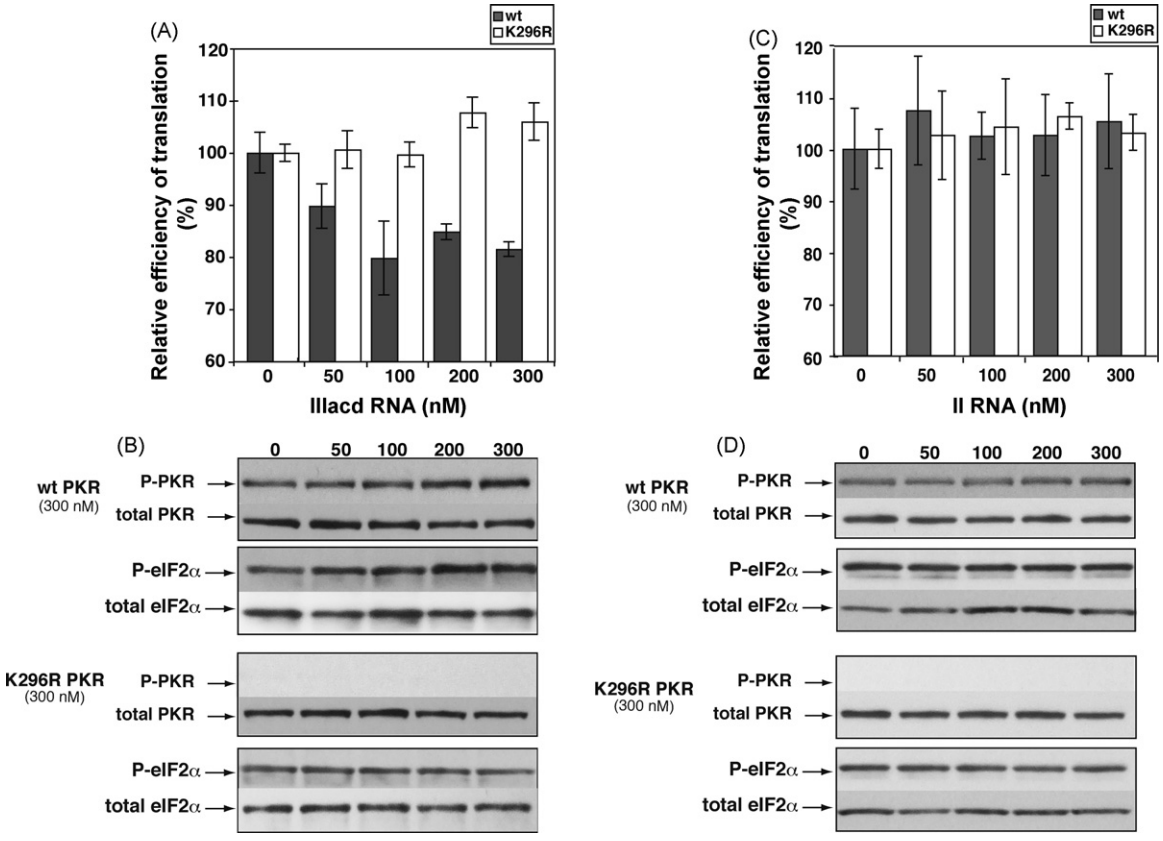

Fig. 5. Inhibition of cap-dependent translation is dose-dependent on HCV RNA. Capped RLuc (50 nM) was incubated with wild-type PKR or K296R PKR (300 nM) and increasing concentrations (0–300 nM) of HCV domain IIIacd (IIIacd) (A and B), or HCV domain II (II) RNA (C and D) in HeLa cell S10 lysate for 1 h at 30 °C. After incubation, portions of the same reaction mixture are used to determine (A and C) translational efficiency (via luciferase assay) and (B and D) phosphorylation state (by Western blotting). Standard deviations are shown from experiments repeated in at least triplicate.

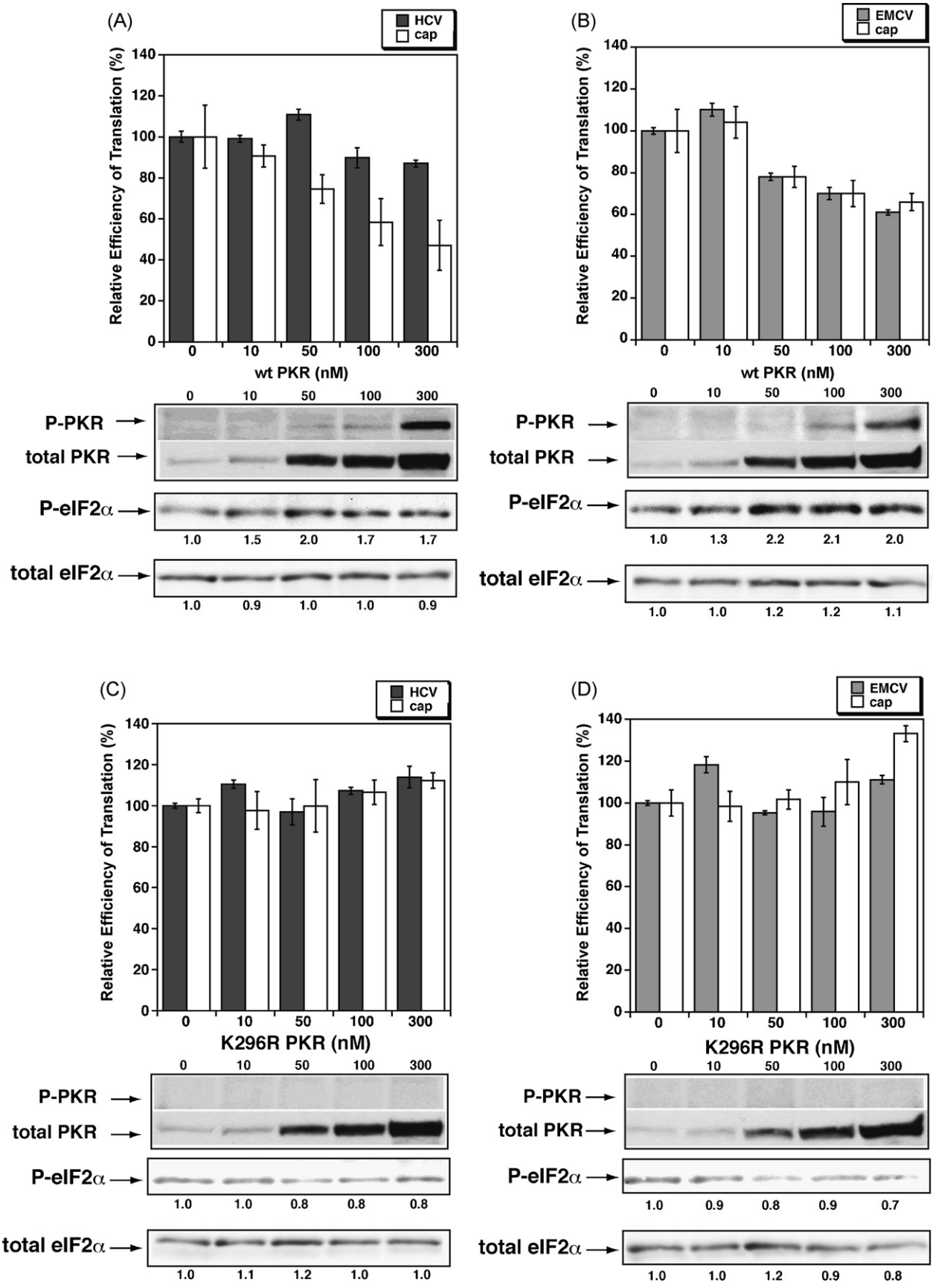

Fig. 6. HCV IRES-dependent translation is not inhibited by PKR autophosphorylation. In all cases the relative efficiency of translation was determined in HeLa cell S10 lysate with a 1 h incubation at 30 °C. After incubation portions of the same reaction mixture are used to determine translational efficiency (via luciferase assay) and phosphorylation state (by Western blotting). Standard deviations are shown from experiments repeated in at least triplicate. Either HCV FLuc (30 nM (A)) or EMCV FLuc (30 nM (B)) and capped RLuc (30 nM) were incubated with increasing amounts of purified wild type PKR. Either HCV FLuc (30 nM (C)) or EMCV FLuc (30 nM (D)) and capped RLuc (30 nM)

We next used nuclear magnetic resonance spectroscopy (NMR) to probe molecular features of the IRES–PKR interaction. ^{1}H–^{15}N-TROSY spectra for dsRBDs in equimolar complex with either HCV IIIacd or HIV TAR (a known activator) were acquired, and each displayed a well-dispersed and resolved spectrum (Fig. 3B). Strikingly, the two overlaid spectra were virtually identical, indicating that a very similar interface within PKR is used to mediate the interaction with either RNA molecule. These regions cluster to specific contiguous surface-exposed regions of the protein, and include both dsRBDs and the linker regions joining them (Kim et al., 2006). We performed identical experiments with HCV IRES and ^{15}N–dsRBDs complex; unfortunately the signal-to-noise ratio was quite poor due to increased line widths of the large (>100 kDa) complex (data not shown). While this observation precludes any definitive conclusions, the cross-peaks were roughly superimposable upon either the IIIacd-dsRBDs or TAR-dsRBDs spectra. These NMR data strongly suggest that PKR dsRBDs bind in a similar manner to either HCV IRES or HIV TAR.

3.4. Phosphorylated PKR has decreased affinity for HCV IRES

Upon phosphorylation of PKR, activator RNA ligands significantly reduced affinity for PKR (McKenna et al., 2007d). Since HCV IRES is an activator of PKR autophosphorylation, we hypothesized that a similar reduction in affinity for HCV IRES should be observed. To test this hypothesis, native gel-shift mobility assays were performed on three activators (HCV IRES, IIIacd, HIV TAR), and one inhibitor (VA_I dsRNA) in the presence of PKR under activating (ATP/$MgCl_2$) conditions at 0- and 60-min time points. Whereas inhibitor RNA did not dissociate from PKR under activating conditions, each of the activator RNAs examined resulted in almost complete complex dissociation (Fig. 3C). These results were dependent on activation, as removal of either ATP or $MgCl_2$ abrogated the effect. Therefore, HCV IRES behaves as a typical activator in terms of its affinity for phosphorylated PKR.

3.5. Cap-dependent translational inhibition by PKR autophosphorylation

Since HCV IRES activates PKR, we next investigated whether this activation process inhibited canonical cap-mediated translation. S10 lysates of HeLa cells were prepared for *in vitro* translation of luciferase reporter constructs. Capped Renilla luciferase RNA (cap-RLuc) was incubated in the presence of HCV IRES RNA and PKR in S10 lysates. After incubation, the efficiency of a cap-dependent translation was measured by the enzymatic activity of Renilla Luciferase. Cap-dependent translation was inhibited with increasing concentration externally added PKR (Fig. 4A). A similar experiment employing a catalytically inactive PKR mutant, K296R, showed no inhibition (Fig. 4A), demonstrating that PKR autophosphorylation is required for the inhibition of cap-dependent translation. Total PKR (endogenous and externally added PKR), phosphorylated PKR, total eIF2α (endogenous), and phosphorylated eIF2α were detected by western blotting (Fig. 4B). The amount of phosphorylated PKR and eIF2α increased only with increasing concentrations of wild-type PKR, and not with K296R PKR addition. A converse experiment confirmed these results. A fixed concentration of wild type or mutant K296R PKR was used for cap-dependent translation, and domain III-oligonucleotide (IIIacd RNA) was added at increasing concentrations. These data show that increasing IIIacd RNA leads to translational inhibition in the presence of wild-type PKR, with no effect on translation in the presence of K296R mutant PKR (Fig. 5A). Western blots suggest that this effect is linked to PKR and eIF2α autophosphorylation (Fig. 5B). The same experiment was performed using domain II RNA, which does not lead to PKR autophosphorylation; increasing concentrations of domain II RNA had no effect on the Cap-dependent translation (Fig. 5C). Western blotting demonstrated that increasing concentrations of domain II RNA did not increase the extent of PKR or eIF2α phosphorylation (Fig. 5D). These results together strongly suggest that HCV IRES RNA inhibits cap-dependent translation through activation of PKR and phosphorylation of eIF2α.

3.6. HCV IRES-dependent translation is not inhibited by PKR autophosphorylation

To explore whether IRES-stimulated activation of PKR inhibits IRES-mediated translation, a fusion reporter of HCV IRES with Firefly luciferase (HCV FLuc) was incubated with PKR and cap-RLuc in S10 lysate. Using this experimental design, the effects of HCV IRES and PKR on both cap- and IRES-mediated translation can be monitored simultaneously in the same reaction. Increasing concentration of PKR inhibits cap-mediated translation (Fig. 6A), as shown above. Western blotting demonstrated increased eIF2α phosphorylation and PKR autophosphorylation (Fig. 6A), indicating that HCV IRES mediates PKR and eIF2α phosphorylation. Interestingly, translation initiated by HCV IRES was not inhibited (Fig. 6A). As a control, we included the highly structured Encephalomyocarditis virus (EMCV) IRES within a reporter construct (EMCV FLuc); EMCV IRES RNA also strongly mediated PKR autophosphorylation (Fig. 6B). A fusion of EMCV IRES with Firefly luciferase was incubated with PKR and cap-RLuc in S10 lysates. Addition of PKR increased the ratio of the inhibition of both EMCV IRES-mediated and cap-dependent translation (Fig. 6B). Western blotting confirmed PKR and eIF2 phosphorylation. As with canonical translation, EMCV IRES-mediated translation was inhibited by eIF2 phosphorylation. These results support a specific lack of response of HCV IRES-mediated translation to eIF2 phosphorylation.

To support the specific role of PKR in the process, we performed identical experiments in HeLa cell S10 lysates using a catalytically inactive mutant of PKR, K296R PKR. As expected, addition of K296R PKR to lysates containing either HCV FLuc and cap-RLuc (Fig. 6C) or EMCV FLuc and cap-RLuc (Fig. 6D) did not lead to attenuation of translation efficiency.

3.7. The release of inhibition by VA_I RNA

To confirm our previous observations, we used VA_I adenoviral RNA that is a potent inhibitor of PKR autophosphorylation (McKenna et al., 2006, 2007b). When HCV FLuc and cap-RLuc were simultaneously incubated in the presence of PKR, inhibition of cap-dependent translation was relieved by addition of an increasing concentration of VA_I RNA (Fig. 7A). In contrast, increasing amounts of VA_I RNA had no effect on the translation initiated by HCV IRES (HCV FLuc), even though PKR and eIF2α phosphorylation decreased (Fig. 7B). As expected, when EMCV FLuc and cap-RLuc were simultaneously incubated in the presence of PKR, an increasing amount of VA_I dsRNA relieved translation inhibition initiated by either EMCV IRES or cap (Fig. 7C), while again PKR and eIF2α phosphorylation decreased (Fig. 7D). These results strongly suggest that the inhibition of cap-dependent translation is caused by phosphorylation in the PKR-eIF2α pathway, and that translation initiated by HCV IRES is not inhibited by phosphorylation of eIF2α.

were incubated with increasing amounts of purified catalytically inactive K296R PKR. The intensities of phosphoryated and total eIF2α were quantified and are indicated beneath each lane (with the intensity set to 1.0 when no external PKR is added).

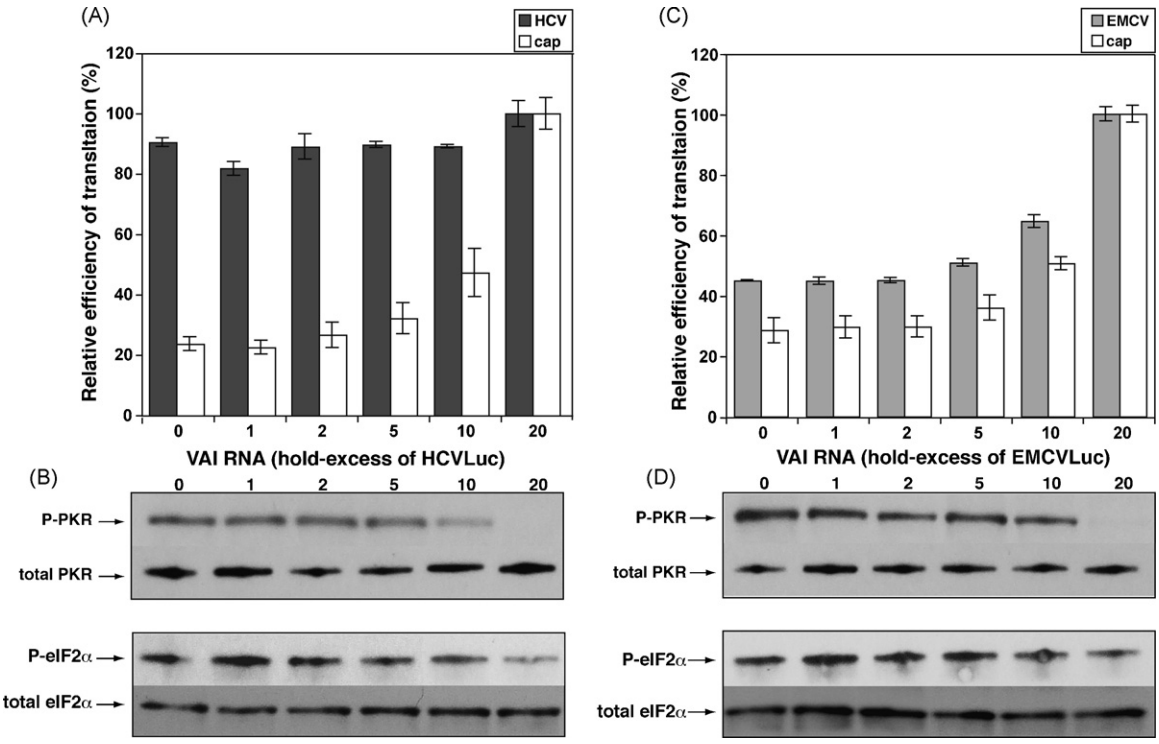

Fig. 7. Release of inhibition by VA_1 RNA. Relative PKR autophosphorylation is presented below each lane. Either HCV FLuc (50 nM (A)) or EMCV FLuc (50 nM (C)) and capped RLuc (50 nM) were incubated with purified PKR (120 nM) and increasing amounts of VA_I RNA in HeLa cell S10 lysate for 1 h at 30 °C. After incubation, portions of the same reaction mixture were used to determine (A and C) translational efficiency (via luciferase assay) and (B and D) phosphorylation state (by Western blotting). Standard deviations are shown from experiments repeated in at least triplicate.

4. Discussion

Large RNAs rich in secondary structure are hallmarks of viral genomes or replication intermediates. The structure of the 350 nt HCV IRES has been previously defined using biochemical and structural methods. The IRES contains three structural domains; domains II and III contain long helical stretches that could potentially activate PKR. Here, we demonstrated that the HCV IRES is a potent activator of recombinant PKR autophosphorylation. We have mapped the high-affinity PKR–IRES RNA interaction to domain III–IV, which also mediates IRES-40S subunit interaction. Domains I and II are dispensable for PKR–IRES interaction, and domain II in isolation binds only weakly to PKR.

NMR and biophysical studies confirmed that the dsRBDs of PKR bind to domain III with affinity and specificity similar to other dsRNA ligands of PKR ($K_D \sim 100$ nM) (Kim et al., 2006; McKenna et al., 2006). The binding site was localized to the lower portion of domain III, below the four-way junction, which contains long stretches of double-helical RNA. The precise secondary structure around the pseudoknot region has not been defined. Neither domains I, II nor IIIb mediate high-affinity interaction with PKR. Domain II binds 80-fold more weakly, and NMR does not reveal a strong interaction between dsRBDs and domain II. Prior structural studies of domain II revealed a long, bent helix, interrupted by a loop E motif near the apical loop, a stretch 13 base pairs of helix that contains 4 non-canonical pairs, that lead to a multinucleotide hinge bulge. Clearly, these helical distortions disrupt the ability of the dsRBDs to make high-affinity contacts. These data underscore the modulatory role of RNA distortions in PKR recognition and affinity for RNA ligands.

Vyas et al. (2003) have previously reported that HCV IRES binds to and inhibits the autophosphorylation PKR, whereas we report here that HCV IRES is a potent activator of PKR under our *in vitro* conditions. This discrepancy may be accounted for by the fact that Vyas et al. tested concentrations of HCV IRES under the K_D (~100 nM) of the PKR–RNA interaction, whereas our assays explored a higher upper threshold. We observed no autophosphorylation under the conditions examined by Vyas et al. (2003). Furthermore, our purified protein was devoid of background phosphorylation (due to co-expression with phosphatase, and re-purification after treatment with phosphatase), whereas Vyas et al. (2003) employed a different purification scheme. In our hands, the presence of HCV IRES RNA led to a greatly increased (20-fold) and level (4.5-fold) of autophosphorylation compared to previously studied viral dsRNA ligands in our laboratory (McKenna et al., 2007d). The increased rate of autophosphorylation may be related to the high charge density of the IRES. Likewise, the high level of PKR autophosphorylation suggests that the IRES–PKR complex is a promiscuous substrate for phosphorylation by PKR. A simple model would predict phosphorylated PKR, which dissociates from the IRES, subsequently phosphorylates PKR–IRES complexes at multiple sites. We are currently investigating these hypotheses in greater mechanistic detail.

Efficient activation of PKR by the HCV IRES leads to rapid phosphorylation of eIF2α. Experiments in S10 extracts showed rapid buildup of PKR and eIF2α phosphorylation in the presence of the IRES. Using simple luciferase translational reporter constructs, we monitored the response of different translation initiation modes to eIF2α phosphorylation. Consistent with many prior observations, the efficiency of cap-mediated translation decreased as the concentration of p-eIF2α increased. Addition of exogenous HCV IRES-stimulated autophosphorylation of PKR and subsequent eIF2α phosphorylation, causing inhibition of cap-mediated translation. Addition of increasing quantities of VA_I RNA, an inhibitor of PKR autophosphorylation that competes for IRES binding, relieved the inhibition of translation. Likewise, translation initiation from a distinct IRES, such as EMCV, was also inhibited by PKR activation and eIF2α phosphorylation, with a similar restoration upon addi-

tion of VA_I RNA. EMCV IRES-mediated initiation requires almost a complete set of initiation factors outside of eIF4E (Pestova et al., 2001). These data confirm the importance of eIF2-GTP concentration for canonical cap-mediated and standard IRES-mediated translation.

HCV uses a distinct mechanism of translation initiation that is not inhibited by eIF2 phosphorylation. The IRES binds directly to the 40S subunit with high affinity, and mediates assembly of a 48S intermediate. GTP hydrolysis, linked to the function of domain II, is required for progression to a stable 80S initiation complex for polyprotein synthesis. GTP hydrolyis, by either or both eIF2 or eIF5B, are required for subunit joining. Our prior data supports this observation (Otto and Puglisi, 2004), but at this stage it is unclear whether eIF2 or eIF5b is the culprit. Our results and those of Robert et al. (2006) show that the IRES-mediated initiation is insensitive to eIF2 phosphorylation, and subsequent buildup of eIF2-GDP. There are also alternate pathways for HCV IRES-mediated initiation. Sarnow and co-workers demonstrated that factor-independent initiation of the IRES can occur under certain conditions (Lancaster et al., 2006), and recent results highlight the absence of a role of eIF2 in IRES-mediated translation (Terenin et al., 2008). The thermodynamic driving force of high-affinity IRES-40S subunit interaction, which positions the start codon near the P-site of the 40S subunit means that the normal search for initiator tRNA codon–anticodon interaction is not needed. The precise role of GTP hydrolysis by eIF2 is not clear, but may be linked to recognition of the correct start codon during scanning. The results presented here suggest a model for the IRES-mediated translation in which hydrolysis of GTP by eIF2 is not an essential step for subsequent subunit joining and initiation. In support, Pestova et al. (2008) have demonstrated that an alternative mode of initiation on the CSFV IRES involving eIF5B in place of eIF2.

Given its upstream position in signal transduction pathways relative to PKR activation, it would be interesting to investigate the upstream activation of RIG-I and TLR-3 by HCV IRES. Recent reports have indicated that both the 3′ untranslated region (especially poly U/C region) and IRES of HCV activate the promoter of IFN-β (Saito et al., 2008). While these investigations are outside the scope of this manuscript, the role of IRES-mediated interactions with these innate immune proteins will be described elsewhere.

Viruses embrace many strategies to circumvent host response. Despite stimulating a strong PKR response, with subsequent and rapid phosphorylation of eIF2, HCV can readily translate its polyprotein in an early step of replication. By evolving a high-affinity ribosome–genomic RNA interaction, which obviates scanning, IRES-mediated translation is resistant to phosphorylation of eIF2. By downregulating host cap-dependent translation, HCV may gain a further selective advantage for replication and propagation. After the preferential translation of viral proteins in an early step of viral replication, translated HCV NS5A and E2 proteins inhibit PKR-activation by binding of "PKR-binding domain" of NS5A and PKR/eIF2α phosphorylation homologous domain (PePHD) of E2 to PKR. This may release the inhibition of both cap- and HCV IRES-dependent translation and permit infected cells to maintain persistent growth and infection that are characteristic of HCV. The effect of HCV IRES, and of NS5A and E2 on PKR-activation, opposes each other. But both may work to the advantage of HCV. Dicer, a central component of the RNA interference mechanism, can digest the HCV IRES into an siRNA of ~22 nucleotides capable of inhibiting the replication of a HCV subgenomic replicon (Wang et al., 2006). However, the RNAi antiviral response is counteracted by the direct interaction between HCV core protein and Dicer. The role of PKR and its interaction with other HCV components (NS5A and E2 proteins, RNAi components, and the genome RNA, etc.) must therefore be explored in more detail.

Acknowledgements

We thank M. Margaris for assistance, and other members of the Puglisi laboratory for their help and advice. We also thank P. Sarnow for useful discussions and reading of the manuscript. We also thank C.M. Rice, P.H. Purcell, J. Bukh and T. Wakita for HCV IRES clones. Supported by NIH AI47365 and GM078346. D.A. Lindhout is supported by the Alberta Heritage Foundation for Medical Research.

References

Bevilacqua, P.C., Cech, T.R., 1996. Minor-groove recognition of double-stranded RNA by the double-stranded RNA-binding domain from the RNA-activated protein kinase PKR. Biochemistry 35, 9983–9994.
Clemens, M.J., Elia, A., 1997. The double-stranded RNA-dependent protein kinase PKR: structure and function. J. Interferon Cytokine Res. 17, 503–524.
Dey, M., Cao, C., Dar, A.C., Tamura, T., Ozato, K., Sicheri, F., Dever, T.E., 2005. Mechanistic link between PKR dimerization, autophosphorylation, and eIF2alpha substrate recognition. Cell 122, 901–913.
Gale Jr., M., Katze, M.G., 1998. Molecular mechanisms of interferon resistance mediated by viral-directed inhibition of PKR, the interferon-induced protein kinase. Pharmacol. Ther. 78, 29–46.
Guidotti, L.G., Chisari, F.V., 2006. Immunobiology and pathogenesis of viral hepatitis. Annu. Rev. Pathol. 1, 23–61.
Honda, M., Beard, M.R., Ping, L.H., Lemon, S.M., 1999. A phylogenetically conserved stem-loop structure at the 5′ border of the internal ribosome entry site of hepatitis C virus is required for cap-independent viral translation. J. Virol. 73, 1165–1174.
Ji, H., Fraser, C.S., Yu, Y., Leary, J., Doudna, J.A., 2004. Coordinated assembly of human translation initiation complexes by the hepatitis C virus internal ribosome entry site RNA. Proc. Natl. Acad. Sci. U.S.A. 101, 16990–16995.
Kieft, J.S., Zhou, K., Grech, A., Jubin, R., Doudna, J.A., 2002. Crystal structure of an RNA tertiary domain essential to HCV IRES-mediated translation initiation. Nat. Struct. Biol. 9, 370–374.
Kieft, J.S., Zhou, K., Jubin, R., Doudna, J.A., 2001. Mechanism of ribosome recruitment by hepatitis C IRES RNA. RNA 7, 194–206.
Kim, I., Liu, C.W., Puglisi, J.D., 2006. Specific recognition of HIV TAR RNA by the dsRNA binding domains (dsRBD1-dsRBD2) of PKR. J. Mol. Biol. 358, 430–442.
Kim, I., Lukavsky, P.J., Puglisi, J.D., 2002. NMR study of 100 kDa HCV IRES RNA using segmental isotope labeling. J. Am. Chem. Soc. 124, 9338–9339.
Kolupaeva, V.G., Pestova, T.V., Hellen, C.U., 2000. An enzymatic footprinting analysis of the interaction of 40S ribosomal subunits with the internal ribosomal entry site of hepatitis C virus. J. Virol. 74, 6242–6250.
Lancaster, A.M., Jan, E., Sarnow, P., 2006. Initiation factor-independent translation mediated by the hepatitis C virus internal ribosome entry site. RNA 12, 894–902.
Locker, N., Easton, L.E., Lukavsky, P.J., 2007. HCV and CSFV IRES domain II mediate eIF2 release during 80S ribosome assembly. EMBO J. 26, 795–805.
Lukavsky, P.J., Otto, G.A., Lancaster, A.M., Sarnow, P., Puglisi, J.D., 2000. Structures of two RNA domains essential for hepatitis C virus internal ribosome entry site function. Nat. Struct. Biol. 7, 1105–1110.
Lukavsky, P.J., Kim, I., Otto, G.A., Puglisi, J.D., 2003. Structure of HCV IRES domain II determined by NMR. Nat. Struct. Biol. 10, 1033–1038.
Lytle, J.R., Wu, L., Robertson, H.D., 2001. The ribosome binding site of hepatitis C virus mRNA. J. Virol. 75, 7629–7636.
McKenna, S.A., Kim, I., Liu, C.W., Puglisi, J.D., 2006. Uncoupling of RNA binding and PKR kinase activation by viral inhibitor RNAs. J. Mol. Biol. 358, 1270–1285.
McKenna, S.A., Kim, I., Puglisi, E.V., Lindhout, D.A., Aitken, C.E., Marshall, R.A., Puglisi, J.D., 2007a. Purification and characterization of transcribed RNAs using gel filtration chromatography. Nat. Protoc. 2, 3270–3277.
McKenna, S.A., Lindhout, D.A., Shimoike, T., Aitken, C.E., Puglisi, J.D., 2007b. Viral dsRNA inhibitors prevent self-association and autophosphorylation of PKR. J. Mol. Biol. 372, 103–113.
McKenna, S.A., Lindhout, D.A., Shimoike, T., Puglisi, J.D., 2007c. Biophysical and biochemical investigations of dsRNA-activated kinase PKR. Methods Enzymol. 430, 373–396.
McKenna, S.A., Lindhout, D.A., Kim, I., Liu, C.W., Gelev, V.M., Wagner, G., Puglisi, J.D., 2007d. Molecular framework for the activation of RNA-dependent protein kinase. J. Biol. Chem. 282, 11474–11486.
Otto, G.A., Lukavsky, P.J., Lancaster, A.M., Sarnow, P., Puglisi, J.D., 2002. Ribosomal proteins mediate the hepatitis C virus IRES-HeLa 40S interaction. RNA 8, 913–923.
Otto, G.A., Puglisi, J.D., 2004. The pathway of HCV IRES-mediated translation initiation. Cell 119, 369–380.
Pestova, T.V., de Breyne, S., Pisarev, A.V., Abaeva, I.S., Hellen, C.U., 2008. eIF2-dependent and eIF2-independent modes of initiation on the CSFV IRES: a common role of domain II. EMBO J. 27, 1060–1072.
Pestova, T.V., Kolupaeva, V.G., Lomakin, I.B., Pilipenko, E.V., Shatsky, I.N., Agol, V.I., Hellen, C.U., 2001. Molecular mechanisms of translation initiation in eukaryotes. Proc. Natl. Acad. Sci. U.S.A 98, 7029–7036.
Pestova, T.V., Shatsky, I.N., Fletcher, S.P., Jackson, R.J., Hellen, C.U., 1998. A prokaryotic-like mode of cytoplasmic eukaryotic ribosome binding to the initiation codon during internal translation initiation of hepatitis C and classical swine fever virus RNAs. Genes Dev. 12, 67–83.

Reynolds, J.E., Kaminski, A., Carroll, A.R., Clarke, B.E., Rowlands, D.J., Jackson, R.J., 1996. Internal initiation of translation of hepatitis C virus RNA: the ribosome entry site is at the authentic initiation codon. RNA 2, 867–878.

Robert, F., Kapp, L.D., Khan, S.N., Acker, M.G., Kolitz, S., Kazemi, S., Kaufman, R.J., Merrick, W.C., Koromilas, A.E., Lorsch, J.R., Pelletier, J., 2006. Initiation of protein synthesis by hepatitis C virus is refractory to reduced eIF2 GTP. Met-tRNA(i)(Met) ternary complex availability. Mol. Biol. Cell 17, 4632–4644.

Saito, T., Owen, D.M., Jiang, F., Marcotrigiano, J., Gale Jr., M., 2008. Innate immunity induced by composition-dependent RIG-I recognition of hepatitis C virus RNA. Nature 454, 523–527.

Shimoike, T., Mimori, S., Tani, H., Matsuura, Y., Miyamura, T., 1999. Interaction of hepatitis C virus core protein with viral sense RNA and suppression of its translation. J. Virol. 73, 9718–9725.

Terenin, I.M., Dmitriev, S.E., Andreev, D.E., Shatsky, I.N., 2008. Eukaryotic translation initiation machinery can operate in a bacterial-like mode without eIF2. Nat. Struct. Mol. Biol. 15, 836–841.

Tsukiyama-Kohara, K., Iizuka, N., Kohara, M., Nomoto, A., 1992. Internal ribosome entry site within hepatitis C virus RNA. J. Virol. 66, 1476–1483.

Vyas, J., Elia, A., Clemens, M.J., 2003. Inhibition of the protein kinase PKR by the internal ribosome entry site of hepatitis C virus genomic RNA. RNA 9, 858–870.

Wang, C., Sarnow, P., Siddiqui, A., 1993. Translation of human hepatitis C virus RNA in cultured cells is mediated by an internal ribosome-binding mechanism. J. Virol. 67, 3338–3344.

Wang, Y., Kato, N., Jazag, A., Dharel, N., Otsuka, M., Taniguchi, H., Kawabe, T., Omata, M., 2006. Hepatitis C virus core protein is a potent inhibitor of RNA silencing-based antiviral response. Gastroenterology 130, 883–892.

Wu, S., Kaufman, R.J., 1997. A model for the double-stranded RNA (dsRNA)-dependent dimerization and activation of the dsRNA-activated protein kinase PKR. J. Biol. Chem. 272, 1291–1296.

Zhao, W.D., Wimmer, E., 2001. Genetic analysis of a poliovirus/hepatitis C virus chimera: new structure for domain II of the internal ribosomal entry site of hepatitis C virus. J. Virol. 75, 3719–3730.